Title:

Extending the known range of glycerol ether lipids in the environment: structural assignments based on MS/MS fragmentation patterns

Author affiliation:

Xiao-Lei Liu [a *], Roger E. Summons [b] , Kai-Uwe Hinrichs [a]

[a] Organic Geochemistry Group, MARUM Center for Marine Environmental Sciences & Dept. of Geosciences, University of Bremen, 28334 Bremen, Germany

[b] Department of Earth, Atmospheric, and Planetary Sciences, Massachusetts Institute of Technology, 77 Massachusetts Avenue, Cambridge, MA 02139-4307, USA

* Corresponding author, Xiao-Lei Liu

Mailing address: Organic Geochemistry Group, MARUM Center for Marine Environmental Sciences & Dept. of Geosciences, University of Bremen, 28334 Bremen, Germany

Tel: 0049-42121865747

Fax: 0049-42121865715

E-mail address: xliu@uni-bremen.de

Author contributions:

X.-L.L, R.E.S. and K.-U.H. designed research; X.-L.L. performed research; X.-L.L, R.E.S. and K.-U.H. analyzed data; X.-L.L. wrote the paper with input from all authors.

The authors declare no conflict of interest.

This is the peer reviewed version of the following article "Liu, X.-L., Summons, R. E. and Hinrichs, K.-U. (2012), Extending the known range of glycerol ether lipids in the environment: structural assignments based on tandem mass spectral fragmentation patterns. Rapid Commun. Mass Spectrom., 26: 2295–2302.", which has been published in final form at doi: 10.1002/rcm.6355.

ABSTRACT

RATIONALE: Glycerol-based alkyl ether lipids are ubiquitous components in marine sediments. In order to explore their structural diversity and biological sources, marine sediment samples from diverse environments were analyzed and the mass spectra of widely distributed, novel glycerol di- and tetraethers were examined systematically.

METHODS: Lipid extracts of twelve globally distributed marine subsurface sediments were analyzed with atmospheric pressure chemical ionization mass spectrometry (APCI/MS). Tandem mass spectra (MS/MS) of compounds were obtained with a quadrupole time-of-flight (qTOF) mass spectrometer.

RESULTS: In addition to the well established isoprenoidal glycerol dialkyl glycerol tetraether (isoprenoidal GDGT) and branched GDGT, suites of novel lipids were detected in all studied samples. These lipids include the following classes of tentatively identified compounds: isoprenoidal glycerol dialkanol diether (isoprenoidal GDD), hydroxylated isoprenoidal GDGT (OH-GDGT), hybrid isoprenoidal/branched GDGT (IB-GDGT), hydroxylated isoprenoidal GDD (OH-GDD), overly branched GDGT (OB-GDGT), sparsely branched GDGT (SB-GDGT) and an abundant H-shaped GDGT with the $[M+H]^+$ ion of *m/z*: 1020 (H-1020).

CONCLUSIONS: Characteristic MS/MS fragmentation patterns provided mass spectral 'fingerprints' for the recognition of diverse and prominent glycerol ether lipids. The ubiquitous distribution and substantial abundance of these glycerol ethers, as well as their structural variability, suggest a significant ecological role of their source organisms in various marine environments.

Key words: Glycerol-based ether lipids, GDGT, marine sediment, HPLC/MS

INTRODUCTION

Isoprenoidal glycerol ethers are characteristic membrane lipids of Archaea, which were initially observed in cultivated extremophiles [1-3] and methanogens. [4, 5] Phylogenetic analysis based on ribosomal RNA and DNA first revealed the prevalence of non-extremophilic archaea in the marine water column and underlying sediments. [6-9] Likewise archaeal ether lipids were discovered to be widespread in marine environments with mesophilic crenarchaeota proposed as the major biological source. [10-13] The most commonly detected isoprenoidal ether lipids are glycerol diphytanyl diether (archaeol) and glycerol dialkyl glycerol tetraethers (isoprenoidal GDGTs), with both groups often being utilized as archaeal biomarkers in modern and geological samples. For example, based on the detection of archaeol and hydroxy-archaeol with anomalously low stable carbon isotopic compositions, Hinrichs et al. [14] identified the presence of methane-oxidizing archaea in marine sediments at methane seeps. Assuming that isoprenoidal GDGTs in sediments are primarily derived from planktonic archaea in the upper water column, the sea surface temperature proxy TEX_{86}, defined by the ratio of isoprenoidal GDGTs with different number of cyclopentane and cyclohexane rings, was established. [15] On the other hand, non-isoprenoidal glycerol ethers, such as branched GDGTs are also common lipid components in sediments. Based on the dominant distribution of branched GDGTs in soils, they are used for assessing soil inputs into marine environments. [16]

During the past decade, the traditional indirect analysis with gas chromatography-mass spectrometry (GC/MS) on ether cleavage products of nonvolatile glycerol ethers has been complemented by high-performance liquid chromatography-mass spectrometry (HPLC/MS) methods capable of analyzing the intact GDGTs, including the intact polar lipid precursors. [17, 18] Although the increased utilization of HPLC/MS resulted in a expansion of the known structural diversity of isoprenoidal and non-isoprenoidal glycerol ether lipids in organisms and natural settings, [e.g. 13] the range of glycerol based ether lipids has been limited to five major series: isoprenoidal diethers, GDGTs, H-shaped GDGTs, glycerol trialkyl glycerol tetraether (GTGT) and branched GDGTs. Ion trap and quadrupole time-of-flight (qTOF) mass spectrometers, which provide additional benefits that come with MS/MS data and accurate mass measurements have, thus, enabled us to conduct the present survey of glycerol ether lipids across a diverse set of marine sediments. These newly recognized classes of lipids and the details of their distributions will provide new information on the microbial inhabitants of these environments.

EXPERIMENTAL

Sample collection and preparation

Twelve globally distributed marine sediments from various environmental settings (Fig. 1) were prepared for analysis as described previously. [19] All sediment samples were freeze-dried and extracted with modified Bligh and Dyer protocol as described by Sturt et al. [18] In addition, two archaeal cultures, i.e., *Methanococcus thermolithotrophicus,* (DSM 2095) *and Methanopyrus kandleri*, (DSM 6324), and one

94 peat bog sample were also analyzed to aid specific lipid characterization (details in SI
95 Text).
96
97 **HPLC/atmospheric pressure chemical ionization/MS analysis**
98 One aliquot of each sample was dissolved in 200 μL hexane/isopropanol [99:1,
99 v/v] for HPLC/MS analysis. Compounds were separated on a Prevail Cyano column
100 (2.1×150 mm, 3 μm; Grace, Deerfield, IL, USA) maintained at 35 °C in an Agilent 1200
101 series HPLC (Agilent Technologies, Waldbronn, Germany). Using a flow rate of 0.25 mL
102 min^{-1}, the gradient of mobile phase was first held for 5 min with 100% of eluent A (n-
103 hexane/isopropanol, 99:1 [v/v]), followed by a linear gradient to 90% of A and 10% B (n-
104 hexane/isopropanol, 90:10 [v/v]) in 20 min, followed by a linear gradient to 100% B at
105 35 min, after hold at 100% B for 5 min. The column was re-equilibrated with 100%
106 eluent A at a flow rate of 0.6 mL min^{-1} for 5 min before the next injection.
107 MS^2 spectra of most of the lipids were generated using an Agilent 6520 qTOF
108 mass spectrometer (Agilent Technologies, Santa Clara, CA, USA) in combination with an
109 Agilent 1200 series HPLC system and an atmospheric pressure chemical ionization
110 (APCI) interface. APCI was set in positive ion mode with nebulizer gas (N_2) pressure 60
111 psi, vaporizer temperature 250°C and drying gas (N_2) temperature 350°C and a flow of
112 4 L min^{-1}. qTOF settings are capillary voltage 1 kV, corona current 5 μA, fragmentor
113 voltage 150 V, skimmer 65 V and octopole 750 V. With an auto MS/MS scanning mode
114 MS^1 records the protonated ions of *m/z* 500-2000. In each cycle three protonated
115 molecules with highest intensity were selected as precursor ions for further MS^2
116 experiments, recorded mass range is *m/z* 100-2000. MS^2 spectra of GTGT-0 and

117 branched GDDs were generated with a ThermoFinnigan LCQ Deca XP Plus ion trap
118 mass spectrometer (ThermoFinnigan, San Jose, CA, USA); APCI settings were as
119 follows: capillary temperature 200 °C, source heater temperature 400 °C, sheath gas
120 flow 30 arbitrary units, source current 5 μA, MS^1 mass range *m/z* 500-1500.
121 Quantification of lipids was achieved with an Agilent 6130 MSD single
122 quadrupole mass spectrometer (Agilent Technologies, Waldbronn, Germany), coupled to
123 an Agilent 1200 series HPLC via multimode ion source set in positive APCI mode. Due
124 to the lack of proper standards, the relative abundance of compounds was calculated
125 based on peak areas without considering their different response factors; relative
126 distributions of compound classes should therefore be viewed semi-quantitative. APCI
127 settings followed the parameters of qTOF, but drying gas (N_2) was at 200°C with a flow
128 of 6 L min^{-1}, capillary voltage 2 kV, and corona current 5 μA. The detector was set using
129 Chemstation software (Agilent, v. B.04.03.54) for selective ion monitoring (SIM) of
130 $[M+H]^+$ ions (*m/z*: 1304, 1302, 1300, 1298, 1296, 1292, 1246, 1244, 1242, 1240, 1236,
131 1218, 1204, 1190, 1176, 1162, 1148, 1134, 1120, 1106, 1092, 1078, 1064, 1050, 1036,
132 1022, 1020, 1008, 994, 980, 966, 653 and with a fragmentor voltage 190 V).
133
134 **RESULTS AND DISCUSSION**
135 More than forty distinct glycerol ether lipids, visualized via LC/MS
136 chromatograms (Fig. 2 and S1), comprising both previously known and newly recognized
137 structures, were present in all twelve samples (Fig. 1). Tentative structural identifications
138 of novel lipids were achieved on the basis of mass spectral data and retention time. The
139 overall distribution of ether lipids is demonstrated by the relative abundance of the 11

140 distinct structural groups identified in the sediments (Fig. 1). Their characteristic MS/MS
141 fragmentation patterns, natural distributions and our ecological interpretations are
142 discussed as follows.
143
144 **Previously known glycerol ethers: Archaeol, GTGT-0, isoprenoidal GDGTs,**
145 **isoprenoidal H-shaped GDGTs and branched GDGTs**
146 We start with briefly describing the range of known components in order to
147 establish the chromatographic and mass spectrometric context for the subsequent
148 discussion of novel components. Under normal-phase LC conditions, archaeol (Ar) is the
149 first eluting glycerol ether lipid with the $[M+H]^+$ ion of *m/z* 653 and a characteristic
150 product ion of *m/z* 373 formed through loss of one phytanyl chain (Fig. S3). The
151 abundance of archaeol in the analyzed marine sediments, as estimated by its response
152 relative to other compounds, is less than 1% of total ether lipids (Fig. 1 and Table S1).
153 Its occurrence in marine sediment is usually attributed to the presence of methanogenic or
154 methanotrophic archaea [20-23] but other sources are conceivable.
155 GTGT-0 containing one biphytanyl and two phytanyl chains as its alkyl units
156 elutes directly after archaeol in normal phase LC (Fig. 2). Because of its special trialkyl
157 tetraether structure, GTGT gives distinctive fragmentation pattern in its MS^2 mass
158 spectrum, [e.g. 24] characterized by a $[M+H]^+$ ion of *m/z* 1304 and product ions of *m/z* 373,
159 931 and 1023 (Fig. S4). The relative abundance of GTGT-0 is rather low, on average, 0.1%
160 of the total suite of glycerol ethers described here (Fig. 1).
161 Accounting for around 55% of total ether lipids (Fig. 1), isoprenoidal GDGTs
162 usually comprise GDGTs with 0-3 cyclopentane rings, the cyclohexane-bearing

crenarchaeol and its regioisomer [13, 15] (Fig. S5A). Their MS^2 spectra are characterized by the protonated molecular ion ($[M+H]^+$) and product ions resulting from loss of one H_2O ($[M+H-18]^+$), one glycerol ($[M+H-74]^+$) and one biphytane unit (Fig. S5B). It has been suggested that isoprenoidal GDGTs preserved in marine sediments are primarily derived from planktonic archaea, but in situ contribution of benthic archaea has also been proposed. [19, 25-28]

Isoprenoidal H-shaped GDGT is an informal designation for GDGT whose two alkyl chains are bridged through a covalent C-C bond. This compound, in our sample set present as H-GDGT-0 in low abundance (~ 0.4% of the total ethers) only in sample ODP201-1229A-22H1 from the Peru margin, has distinctive MS^2 behavior under LC/APCI/MS [e.g. 24] that differs from GDGTs in that there are only product ions corresponding to loss of H_2O and a glycerol unit; no ions resulting from the loss of a single alkyl chain (Fig. S6).

Branched GDGTs are non-isoprenoidal glycerol tetraethers with 13,16-dimethyl or 5,13,16-trimethyl octacosanyl moieties. The 1,2-di-O-alkyl-*sn*-glycerol configuration of branched GDGTs implies a bacterial rather than archaeal origin. [29, 30] The branched GDGTs account for ~10% of the total glycerol ether lipids in our samples (Fig. 1). Three branched GDGTs are prominent in both marine and terrestrial environments [16, 30] and comprise homologs with $[M+H]^+$ of *m/z* 1022, 1036 and 1050 that differ in their degree of methylation rather than alkyl chain length (see molecular structures in Figs. 2 & S1 and Figs. 3 & S2).

OB- and SB-GDGTs

186 Detailed evaluation of the mass spectra of the branched GDGTs has exposed two
187 related series of compounds that are also interpreted to be based on octacosanyl chains
188 but in comparison to the branched GDGTs with either higher (overly branched, OB-
189 GDGTs) or lower degrees (sparsely branched, SB-GDGTs) of methylation (Fig. 3 and
190 Fig. S2). OB- and SB-GDGTs were present in all samples with a relative abundance of ~
191 3% on average. Their glycerol tetraether skeleton yields characteristic product ions in
192 MS^2 through loss of H_2O, glycerol and one alkyl unit (Fig. 3 and S2). The product ions
193 resulting from loss of a single alkyl chain provide clues to the carbon number of each
194 alkyl moiety of the OB- and SB-GDGTs. Although exact methylation patterns remain to
195 be elucidated, the mass spectral evidence of the compound series strongly suggests that
196 methylation occurred successively on alternative alkyl moieties, from the smallest
197 branched GDGT ($[M+H]^+$ of *m/z* 1022) to the largest OB-GDGT ($[M+H]^+$ of *m/z* 1134)
198 (Fig. 3 and Fig. S2). GC/MS analysis of the hydrocarbons released by ether cleavage and
199 subsequent reduction (SI Text) indicates that structural complexity is due to multiple sites
200 of methylation along the carbon chains (Fig. 4 and S7). Based on the evidence at hand,
201 we tentatively illustrate the OB- and SB-GDGTs (Fig. 2 and 3) as homologues in which
202 successive methylations result in partially isoprenoidal structures (see structures in Figs.
203 2 & S1 and Figs. 3 & S2). Verification of exact structures of these components will
204 require their isolation and NMR analysis (cf. Liu et al., 2012 [32]). Biological sources of
205 OB- and SB-GDGTs and the biosynthetic mechanisms for methylation or demethylation
206 of alkyl moieties are currently unknown. However, the observed relationships between
207 the degree of methylation of the branched GDGTs in soil, mean annual air temperature

208 and soil *p*H [31] imply that environmental factors may influence the distribution of OB-
209 and SB-GDGTs in the marine realm.
210
211 **IB-GDGTs**
212 Tentatively identified hybrid isoprenoidal/branched (IB)-GDGTs possess alkyl
213 chains that combine widely considered attributes characteristic of both archaea (phytanyl
214 moiety) and bacteria (methylated-alkyl moiety). IB-GDGTs co-elute with isoprenoidal
215 GDGT-3 and crenarchaeol (Fig. 2). Based on interpretation of methylation patterns and
216 relative retention time, we tentatively assign a triacontanyl chain with various degrees of
217 methylation to this class. Indeed, the presence of one compound ($[M+H]^+$, *m/z* 1190) of
218 this series was previously reported for multiple depositional settings. [13] Detailed analysis
219 of our LC/MS data reveals additional IB-GDGT analogues with both higher and lower
220 degrees of methylation. In total, seven IB-GDGTs have been detected (Fig. 3 and S2).
221 The lowest molecular weight IB-GDGT has the same protonated molecular ion ($[M+H]^+$,
222 *m/z* 1134) as the largest OB-GDGT, while they are chromatographically distinct (Fig. 3
223 and S2), consistent with different alkyl chain lengths and methylation patterns. As for the
224 OB-GDGTs, the precise structures of the IB-GDGTs remain unresolved although the
225 differences within each series must lie in the patterns of methylation. Under LC/MS/MS,
226 the product ions resulting from loss of a single alkyl chain of IB-, OB- and branched
227 GDGTs show that increasing degrees of methylation occurs on alternate alkyl chains. In
228 other words, if one compound possesses two more methyl groups than another compound
229 within the series of IB-GDGTs, it carries one additional methyl group at each alkyl
230 moiety. One exception is the IB-GDGT with $[M+H]^+$ of *m/z* 1190. For this compound

231 the two product ions formed by the alkyl chains differ by 28 m/z (i.e., m/z 673.651 and
232 701.683, of IB-GDGT 1190 in Fig. 3 and S2). This could either reflect a difference in
233 alkyl chain length as suggested previously by Schouten et al. for a related compound [13],
234 or two more methyl groups on one alkyl moiety.
235 IB-GDGTs were detected in all samples at an average abundance of ~1.6% of
236 total ether lipids. Isolation of IB-GDGTs via preparative LC and subsequent NMR
237 analyses are expected to reveal their exact structures in the future. To date, the biological
238 source of IB-GDGT remains elusive.
239
240 **OH-GDGTs**
241 Hydroxylated analogues of known isoprenoidal GDGTs were detected in all
242 sediments with the average abundance of ~ 3% of total ether lipids (Fig. 1); the
243 distributions and detailed structural analysis of the mono-hydroxyl derivatives have been
244 described in a separate report. [32] The additional hydroxyl groups of OH-GDGTs result in
245 increased polarity and later elution under normal phase LC conditions compared to the
246 isoprenoidal GDGTs (Fig. 2). Under APCI conditions, OH-GDGTs readily dehydrate
247 yielding $[M+H-18]^+$ ions for monohydroxylated and $[M+H-36]^+$ ions for dihydroxylated
248 GDGTs (Fig. 5). The fragmentation patterns evident in the MS^2 spectra of GDGT-0,
249 OH-GDGT-0 and 2OH-GDGT-0 (Fig. S9) all confirm that hydroxylated biphytanes are
250 preferentially lost and that for 2OH-GDGT, both hydroxyl groups are located at the same
251 biphytane moiety.
252 OH-GDGTs are present in all analyzed samples. They have ring distributions
253 distinct from those of the co-occurring isoprenoidal GDGTs. [32] Isomerism in the OH-

GDGTs, identified on the basis of the distribution and retention times of products in acid hydrolyzed TLE of a *Methanococcus thermolithotrophicus* culture (Fig. S10) confirms that the mono- and dihydroxyl GDGTs that normally occur in marine sediments are compounds (2) and (5). However, other isomers present in the lipids of *M. thermolithotrophicus* are not detected in sediments. Further, their IPL precursors, including 2Gly-OH-GDGT, are detected with remarkable abundance in the anoxic Black Sea water column, [33] at methane seep sites, [34] in subsurface sediments; [27, 32] in these previous studies they were designated as H341-GDGT or 2Gly-GDGT+18. Diglycosidic OH-GDGTs were also found in the planktonic crenarchaeote *Candidatus Nitrosopumilus maritimus* [35] (designated as unknown intact isoprenoidal GDGT with one hexose plus 180 Da head group) and the euryarchaeote *Methanococcus thermolithotrophicus*, [32] indicating that they are not limited to one archaeal kingdom. Their substantial abundance in marine environments suggests that OH-GDGTs may harbor potential as taxonomic biomarkers and geobiological proxies.

GDDs

GDDs appear to be derivatives of GDGTs lacking one glycerol moiety. [36] Here we introduce OH-GDDs and branched GDDs as relatives of the previously described ubiquitous series of isoprenoidal GDDs. [36] Isoprenoidal GDDs and OH-GDDs co-occur with their corresponding isoprenoidal GDGTs and OH-GDGTs in all samples (Fig. 5). Likewise, branched GDDs (Fig. S11) are detected in settings where branched GDGTs are abundant. GDDs are more polar than the corresponding GDGTs (Fig. 2) and are usually less abundant (Fig. 1). Characteristic product ions in the MS^2 spectra of GDD-

277 crenarchaeol, GDD-0, OH-GDD-0 and 2OH-GDD-0 are shown in Fig. S12. As an
278 analogue to the product ions with *m/z* 743 in the MS^2 spectra of 2OH-GDGT-0 (Fig. S9),
279 2OH-GDD-0 (Fig. S12) possesses a major product ion at 669 *m/z* that consists of a single
280 glycerol moiety linked to a saturated biphytane, thus indicating the presence of both
281 hydroxyl groups on a single biphytanyl group.
282 Isoprenoidal GDGTs and GDDs exhibit similar cyclization patterns, strongly
283 suggesting related biological sources for these two lipid groups. The unique bipolar
284 structure of GDDs and their coexistence with corresponding GDGTs in marine sediments
285 and archaeal cultures identify GDDs as either functional lipids or biosynthetic
286 intermediates. Their prevalence as products of diagenesis or even artificial formation
287 during sample preparation appears rather unlikely due to the presence of hydroxylated
288 isoprenoidal GDDs because cleavage of two ether bonds requires chemically harsher
289 conditions than dehydration of a labile tertiary hydroxyl group. The ubiquitous
290 distribution and remarkable abundance of isoprenoidal GDDs, which account on average
291 for 11.7% of the total glycerol ether lipids (Fig. 1) in our sample set, identify them as
292 potential molecular proxies once their physiological role is better understood. One current
293 hypothesis is that they are diagnostic of lipid recycling mediated by benthic archaea. [37]
294
295 **Novel H-shaped GDGTs**
296 In addition to the previously reported structures, such as H-shaped GDGTs with
297 0-4 cyclopentane rings, [38] we also detected novel H-shaped GDGTs with extra
298 methylation on the hydrocarbon chains (SI Text and Fig. S6). Additionally, we identified
299 the ubiquitous compound denoted H-1020 (Fig. 2 and S1) as having an H-shaped

300 structure (Fig. S13). This compound is remarkably abundant at ~ 13% of total ether lipids
301 in our sample set. The source of H-1020 remains unknown but its high abundance in
302 many marine settings indicates that formation of a H-shaped structure in membrane-
303 spanning lipids has a physiological purpose other than survival at high temperatures. [38]
304

305 ## CONCLUSIONS

306 The detection and recognition of novel glycerol ether lipids in marine sediments
307 by means of LC/MS with APCI has revealed an unexpected diversity of membrane lipid
308 derivatives produced by both Archaea and Bacteria. A large proportion of these
309 compounds has previously evaded detection. The identification of both isoprenoidal and
310 branched-alkyl GDDs shows, for the first time, the existence of bipolar diethers with
311 three free hydroxyl groups while the OH-GDGT tetraether is the first described analogue
312 of the well-known hydroxy diethers. More complex structures include the methylation
313 series of IB-, OB-, SB- and branched GDGTs and methylated H-shaped GDGTs.
314 Although the exact structures of IB-, OB- and SB-GDGTs and H-1020 remain to be
315 resolved in future research, their widespread nature and high abundance in marine
316 sediments shows that their biological sources are important members of marine
317 ecosystems. The mass spectral data presented here serves as a 'fingerprint' of each
318 compound and will facilitate future analyses and especially investigation of these sources
319 of numerous novel compounds that occur ubiquitously in marine sediments.
320

321 ## Acknowledgments

This research used samples provided by the Ocean Drilling Program (ODP) and the Integrated Ocean Drilling Program (IODP), which are sponsored by the US National Science Foundation and participating countries under management of Joint Oceanographic Institutions (JOI), Inc. We are grateful to the participating scientists and ship crews of the IODP Expedition 311, the ODP Legs 160, 201 and 204, RV Meteor cruise M76/1 and Sonne cruise SO147. Prof. Michael Thomm, Dr. Emma Gagen, Manuela Baumgartner and Prof. Karl Stetter provided the archaeal cultures. This study was funded by *Deutsche Forschungsgemeinschaft* (DFG, Germany) through the international graduate college EUROPROX for a scholarship to X.-L.L. Additional funding to X.L.-L. was provided to ERC Advanced Grant DARCLIFE (PI K-UH) and awards from the US National Science Foundation (# ETBC OCE-0849940 and ARC-0806228) and from the NASA Astrobiology Institute (# NNA08CN84A) to R.E.S.

References

1. M. Kates, P. S. Sastry, L. S. Yengoyan. Isolation and characterization of a diether analog of phosphatidylglycerophosphate from *Halobacterium cutirubrum*. *Biochim. Biophys. Acta* **1963**, *70*, 705.
2. M. De Rosa, S. De Rosa, A. Gambacorta, J. D. Bu'lock. Isoprenoid triether lipids from Caldariella. *Phytochemistry* **1976**, *15*, 1995.
3. T. A. Langworthy. Long-chain diglycerol tetraethers from *Thermoplasma Acidophilum*. *Biochim. Biophys. Acta* **1977**, *487*, 37.
4. R. A. Makula, M. E. Singer. Ether-containing lipids of methanogenic bacteria. *Biochem. Biophys. Res. Commun.* **1978**, *82*, 716.
5. T. G. Tornabene, T. A. Langworthy. Diphytanyl and dibiphytanyl glycerol ether lipids of methanogenic archaebacteria. *Science* **1979**, *203*, 51.
6. E. F. DeLong. Archaea in coastal marine environments. *Proc. Natl. Acad. Sci. USA.* **1992**, *89*, 5685.
7. J. A. Fuhrman, K. McCallum, A. A. Davis. Novel major archaebacterial group from marine plankton. *Nature* **1992**, *356*, 148.
8. C. Vetriani, A. L. Reysenbach, J. Dore. Recovery and phylogenetic analysis of archaeal rRNA sequences from continental shelf sediments. *FEMS Microbiol. Lett.* **1998**, *161*, 83.
9. C. Vetriani, H. W. Jannasch, B. J. MacGregor, D. A. Stahl, A. L. Reysenbach. Population structure and phylogenetic characterization of marine benthic archaea in deep-sea sediments. *Appl. Environ. Microbiol.* **1999**, *65*, 4375.
10. M. J. L. Hoefs, S. Schouten, J. W. De Leeuw, L. L. King, S. G. Wakeham, J. S. Sinninghe Damsté. Ether lipids of planktonic archaea in the marine water column. *Appl. Environ. Microbiol.* **1997**, *63*, 3090.
11. E. F. DeLong, L. L. King, R. Massana, H. Cittone, A. Murray, C. Schleper, S. G. Wakeham. Dibiphytanyl ether lipids in nonthermophilic crenarchaeotes. *Appl. Environ. Microbiol.* **1998**, *64*, 133.
12. S. Schouten, M. J. L. Hoefs, M. P. Koopmans, H. Bosch, J. S. Sinninghe Damsté. Structural characterization, occurrence and fate of archaeal ether-bound acyclic and cyclic biphytanes and corresponding diols in sediments. *Org. Geochem.* **1998**, *29*, 1305.
13. S. Schouten, E. C. Hopmans, R. D. Pancost, J. S. Sinninghe Damsté. Widespread occurrence of structurally diverse tetraether membrane lipids: Evidence for the ubiquitous presence of low-temperature relatives of hyperthermophiles. *Proc. Natl. Acad. Sci. USA.* **2000**, *97*, 14421.
14. K. -U. Hinrichs, J. M. Hayes, S. P. Sylva, P. G. Brewer, E. F. DeLong. Methane-consuming archaebacteria in marine sediments. *Nature* **1999**, *398*, 802.
15. S. Schouten, E. C. Hopmans, E. Schefuß, J. S. Sinninghe Damsté. Distributional variations in marine crenarchaeotal membrane lipids: a new tool for reconstructing ancient sea water temperatures? *Earth Planet. Sci. Lett.* **2002**, *204*, 265.
16. E. C. Hopmans, J. W. H. Weijers, E. Schefuß, L. Herfort, J. S. Sinninghe Damsté, S. Schouten. A novel proxy for terrestrial organic matter in sediments based on branched and isoprenoid tetraether lipids. *Earth Planet. Sci. Lett.* **2004**, *224*, 107.

17. E. C. Hopmans, S. Schouten, R. D. Pancost, M. T. J. van der Meer, J. S. Sinninghe Damsté. Analysis of intact tetraether lipids in archaeal cell material and sediments by high performance liquid chromatography/atmospheric pressure chemical ionization mass spectrometry. *Rapid. Commun. Mass Spectrom.* **2000**, *14*, 585.
18. H. F. Sturt, R. E. Summons, K. Smith, M. Elvert, K. -U. Hinrichs. Intact polar membrane lipids in prokaryotes and sediments deciphered by high-performance liquid chromatography/electrospray ionization multistage mass spectrometry-new biomarkers for biogeochemistry and microbial ecology. *Rapid. Commun. Mass Spectrom.* **2004**, *18*, 617.
19. X. -L. Liu, J. S. Lipp, K. -U. Hinrichs. Distribution of intact and core GDGTs in marine sediments. *Org. Geochem.* **2011**, *42*, 368.
20. K. -U. Hinrichs, R. E. Summons, O. Victoria, S. P. Sylva, J. M. Hayes. Molecular and isotopic analysis of anaerobic methane-oxidizing communities in marine sediments. *Org. Geochem.* **2000**, *31*, 1685.
21. R. D. Pancost, J. S. Sinninghe Damste´, S. de Lint, M. J. E. C. van der Maarel, J. C. Gottschal, Medinaut Shipboard Scientific Party. Biomarker evidence for widespread anaerobic methane oxidation on Mediterranean sediments by a consortium of methanogenic archaea and bacteria. *Appl. Environ. Microbiol.* **2000**, *66*, 1126.
22. R. D. Pancost, E. C. Hopmans, J. S. Sinninghe Damsté, MEDINAUT Shipboard Scientific Party. Archaeal lipids in Mediterranean cold seeps: molecular proxies for anaerobic methane oxidation. *Geochim. Cosmochim. Acta* **2001**, *65*, 1611.
23. P. E. Rossel, J. S. Lipp, H. F. Fredricks, J. Arnds, A. Boetius, M. Elvert, K. -U. Hinrichs. Intact polar lipids of anaerobic methanotrophic archaea and associated bacteria. *Org. Geochem.* **2008**, *39*, 992.
24. C. S. Knappy, J. P. J. Chong, B. J. Keely. Rapid Discrimination of Archaeal Tetraether Lipid Cores by Liquid Chromatography–Tandem Mass Spectrometry. *J. Am. Soc. Mass Spectrom.* **2009**, *20*, 51.
25. J. F. Biddle, J. S. Lipp, M. A. Lever, K. G. Lloyd, K. B. Sørensen, R. Anderson, H. F. Fredricks, M. Elvert, T. J. Kelly, D. P. Schrag, M. L. Sogin, J. E. Brenchley, A. Teske, C. H. House, K. -U. Hinrichs. Heterotrophic archaea dominate sedimentary subsurface ecosystems off Peru. *Proc. Natl. Acad. Sci. USA.* **2006**, *103*, 3846.
26. J. S. Lipp, Y. Morono, F. Inagaki, K. -U. Hinrichs. Significant contribution of Archaea to extant biomass in marine subsurface sediments. *Nature* **2008**, *454*, 991.
27. J. S. Lipp, K. -U. Hinrichs. Structural diversity and fate of intact polar lipids in marine sediments. *Geochim. Cosmochim. Acta* **2009**, *73*, 6816.
28. S. Schouten, J. J. Middelburg, E. C. Hopmans, J. S. Sinninghe Damsté. Fossilization and degradation of intact polar lipids in deep subsurface sediments: A theoretical approach. *Geochim. Cosmochim. Acta* **2010**, *74*, 3806.
29. J. S. Sinninghe Damsté, E. C. Hopmans, R. D. Pancost, S. Schouten, J. A. J. Geenevasen. Newly discovered non-isoprenoid glycerol dialkyl glycerol tetraether lipids in sediments. *Chem. Commun.* **2000**, 1683.
30. J. W. H. Weijers, S. Schouten, E. C. Hopmans, J. A. J. Geenevasen, O. R. P. David, J. M. Coleman, R. D. Pancost, J. S. Sinninghe Damsté. Membrane lipids of mesophilic anaerobic bacteria thriving in peats have typical archaeal traits. *Environ. Microbiol.* **2006**, *8*, 648.

31. J. W. H. Weijers, S. Schouten, J. C. van den Donker, E. C. Hopmans, J. S. Sinninghe Damsté. Environmental controls on bacterial tetraether membrane lipid distribution in soils. *Geochim. Cosmochim. Acta* **2007**, *71*, 703.
32. X. -L. Liu, J. S. Lipp, J. H. Simpson, Y. -S. Lin, R. E. Summons, K. -U. Hinrichs. Mono- and dihydroxyl Glycerol Dibiphytanyl Glycerol Tetraethers in marine sediments: identification of both core and intact polar lipid forms. *Geochim. Cosmochim. Acta* **2012**, *89*, 102.
33. F. Schubotz, S. G. Wakeham, J. S. Lipp, H. F. Fredricks, K. -U. Hinrichs. Detection of microbial biomass by intact polar membrane lipid analysis in the water column and surface sediments of the Black Sea. *Environ. Microbiol.* **2009**, *11*, 2720.
34. P. E. Rossel, M. Elvert, A. Ramette, A. Boetius, K. -U. Hinrichs. Factors controlling the distribution of anaerobic methanotrophic communities in marine environments: evidence from intact polar lipids. *Geochim. Cosmochim. Acta* **2011**, *75*, 164.
35. S. Schouten, E. C. Hopmans, M. Bass, H. Boumann, S. Standfest, M. Könneke, S. A. Stahl, J. S. Sinninghe Damste. Intact membrane lipids of "Candidatus Nitrosopumilus maritimus", a cultivated representative of the cosmopolitan mesophilic group I Crenarchaeota. *Appl. Environ. Microbiol.* **2008**, *74*, 2433.
36. X. -L. Liu, J. S. Lipp, J. Schröder, R. E. Summons, K. -U. Hinrichs. Isoprenoidal glycerol dialkanol diethers: a series of novel archaeal lipids in marine sediments. *Org. Geochem.* **2012**, *43*, 50.
37. Y. Takano, Y. Chikaraishi, O. N. Ogawa, H. Nomaki, Y. Morono, F. Inagaki, H. Kitazato, K. -U. Hinrichs, N. Ohkouchi. Sedimentary membrane lipids recycled by deep-sea benthic archaea. *Nature Geosci.* **2010**, *3*, 858.
38. S. Schouten, M. Baas, E. C. Hopmans, A. Reysenbach, J. S. Sinninghe Damsté. Tetraether membrane lipids of Candidatus ''*Aciduliprofundum boonei*'', a cultivated obligate thermoacidophilic euryarchaeote from deep-sea hydrothermal vents. *Extremophiles* **2008**, *12*, 119.

Figure captions

Figure 1. Distribution of 11 groups of detected glycerol ether lipids in 12 marine subsurface sediments.

The relative abundance (%) of 11 structural groups in each sample presented in the form of a quasi-3D histogram. Detailed sample information and raw data are presented in Table S1. The map shows the location of sampling sites.

Figure 2. LC/APCI/MS chromatogram showing the distribution of glycerol ether lipids in sample ODP201-1229D-4H4, Peru Margin.

A color-coded composite chromatogram (generated by Agilent 6130 MSD single quadrupole MS) showing the elution order and structures of representative compounds. Co-eluting and less abundant species components are shown as insets below the main chromatogram. The signals for Ar (archaeol) and GTGT-0 have been amplified by 40 times, IB-GDGTs, OB-GDGTs, SB-GDGTs, 2OH-GDGT and OH-GDDs by 100 times. H-GDGT-0 and 2OH-GDD were not detected in this sample and an asterisk indicates their elution positions based on the chromatograms of other samples. A full version of this figure (Fig. S1) with diagnostic $[M+H]^+$ values and molecular structures of all detected lipids is provided in Supporting Information.

Figure 3. Tentative identification of IB-, OB-, branched and SB-GDGTs by MS^2 spectra (qTOF)**.**

Extracted ion chromatograms (EIC) showing the different compound classes in their specific mass windows (left panel). Product ion (MS^2) spectra of representative compounds show the characteristic product ions (numbers in red, product ions resulting from the loss of one alkyl chain) used to identify each structure (right panel). Due to the low intensity and interference caused by co-elution, the MS^2 spectra of IB-GDGTs (*m/z* 1148 and 1134) and SB-GDGTs are not shown here. Partial MS^2 spectra of IB-GDGTs are amplified in separate windows. Putative structures of the lowest molecular weight IB-GDGT and the highest molecular weight OB-GDGT

484 (*m/z* 1134, I and II) are illustrated in the central box for comparative purposes. A full
485 version of this figure (Fig. S2) with MS^2 spectra of other lipids is provided in
486 Supporting Information.
487
488 **Figure 4. GC/MS of ether cleavage released hydrocarbons.**
489 The TIC (total ion chromatogram) showing the composition of hydrocarbons
490 released from B-, OB-, IB- and isoprenoidal GDGTs. Peak 1 is 13,16-dimethyl
491 octacosane, 2a~e are trimethyl octacosanes, 3a and b are tetramethyl octacosanes, 4a and
492 b are pentamethyl octacosanes and 5a and b are hexamethyl octacosanes. 6a and b are
493 hydrocarbons released from IB-GDGT 1190 and are tentatively assigned as
494 pentamethyltriacontane and heptamethyltriacontane, respectively (Fig. S8). The mass
495 spectra of labeled peaks are shown in Supporting Information, Fig. S7 and S8.
496
497 **Figure 5. LC/APCI/MS chromatograms (MSD) of M76/1 GeoB12806-2.**
498 EIC showing the distribution of isoprenoidal GDGTs, OH-GDGTs and their
499 corresponding GDDs.
500

501 **Figures**

502

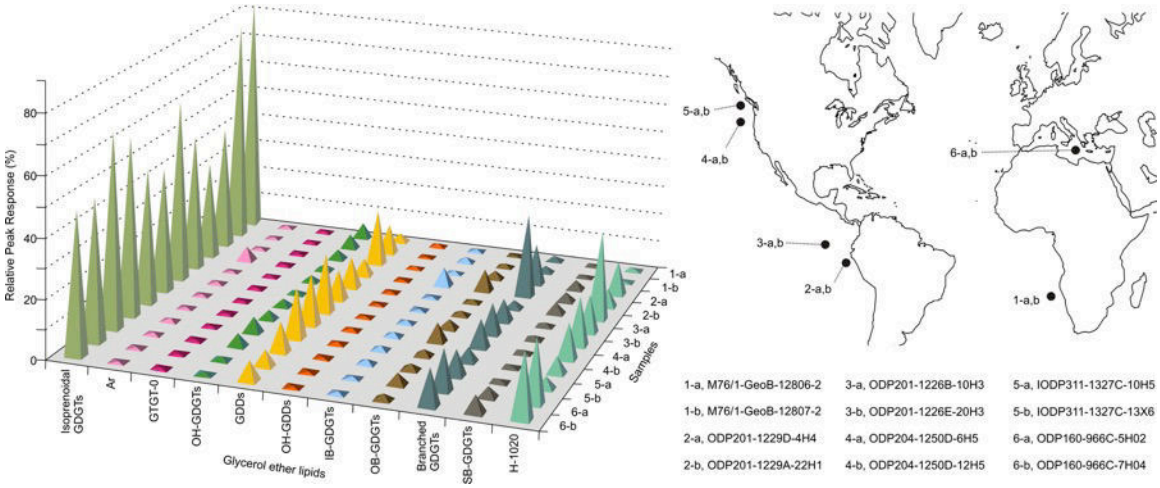

503

504 Fig. 1

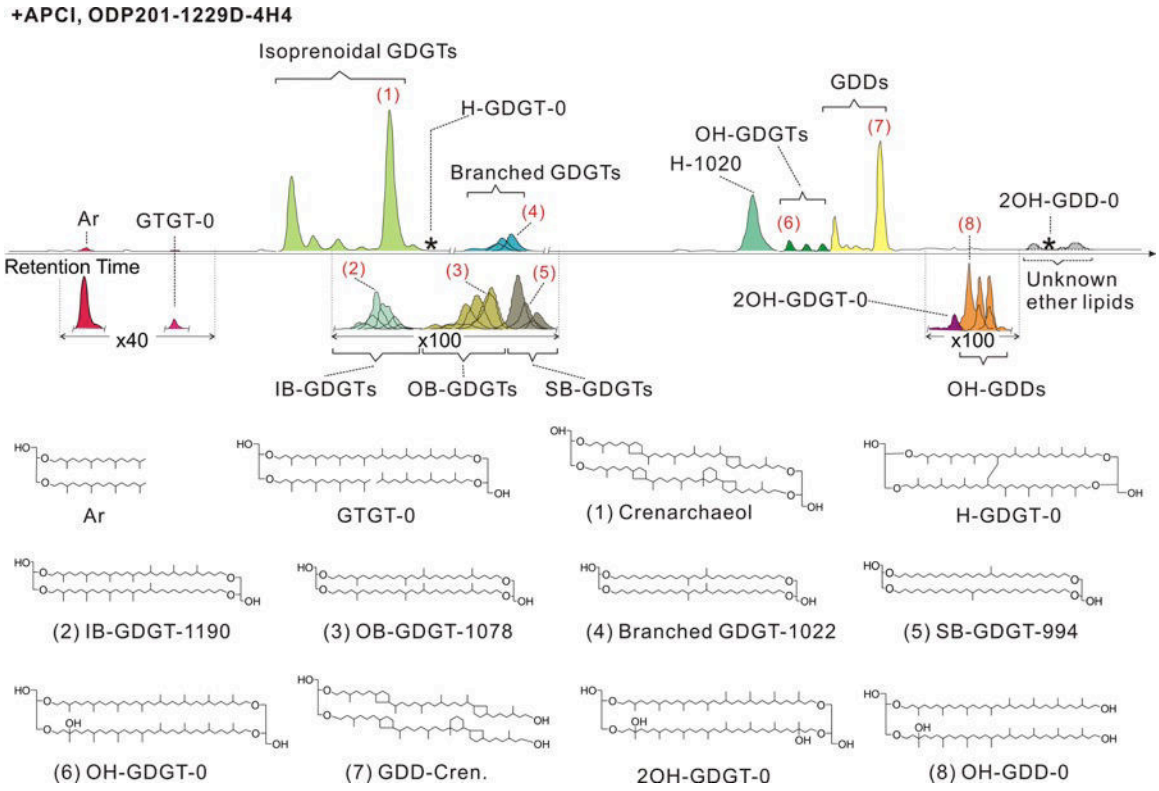
+APCI, ODP201-1229D-4H4
Isoprenoidal GDGTs
(1)
H-GDGT-0
Branched GDGTs
(4)
GDDs
(7)
OH-GDGTs
H-1020
(6)
2OH-GDD-0
(8)
Ar
GTGT-0
Retention Time
x40
(2)
(3)
(5)
x100
IB-GDGTs
OB-GDGTs
SB-GDGTs
2OH-GDGT-0
x100
Unknown
ether lipids
OH-GDDs
Ar
GTGT-0
(1) Crenarchaeol
H-GDGT-0
(2) IB-GDGT-1190
(3) OB-GDGT-1078
(4) Branched GDGT-1022
(5) SB-GDGT-994
(6) OH-GDGT-0
(7) GDD-Cren.
2OH-GDGT-0
(8) OH-GDD-0

Fig. 2

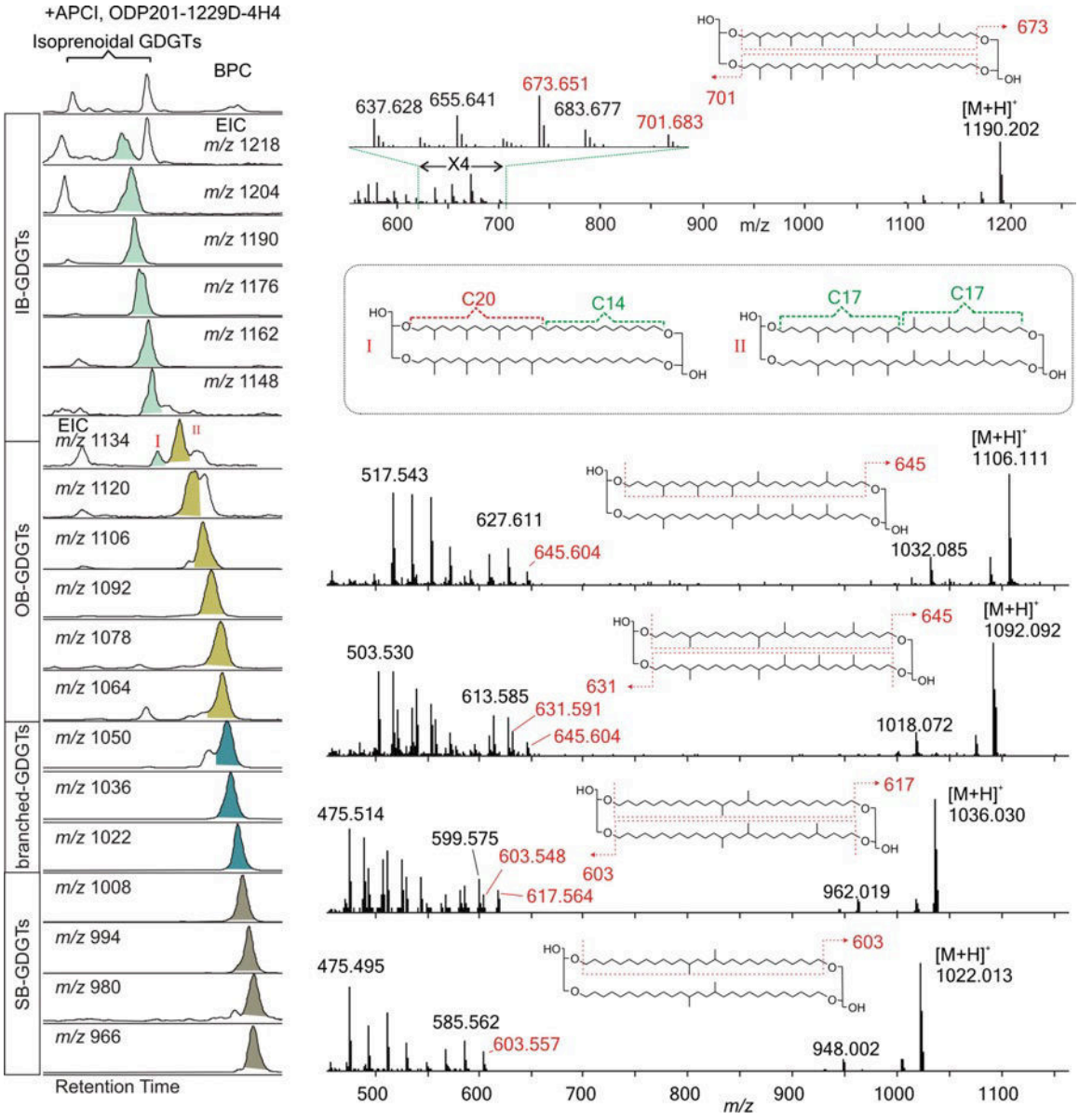

509

510 Fig. 3

511

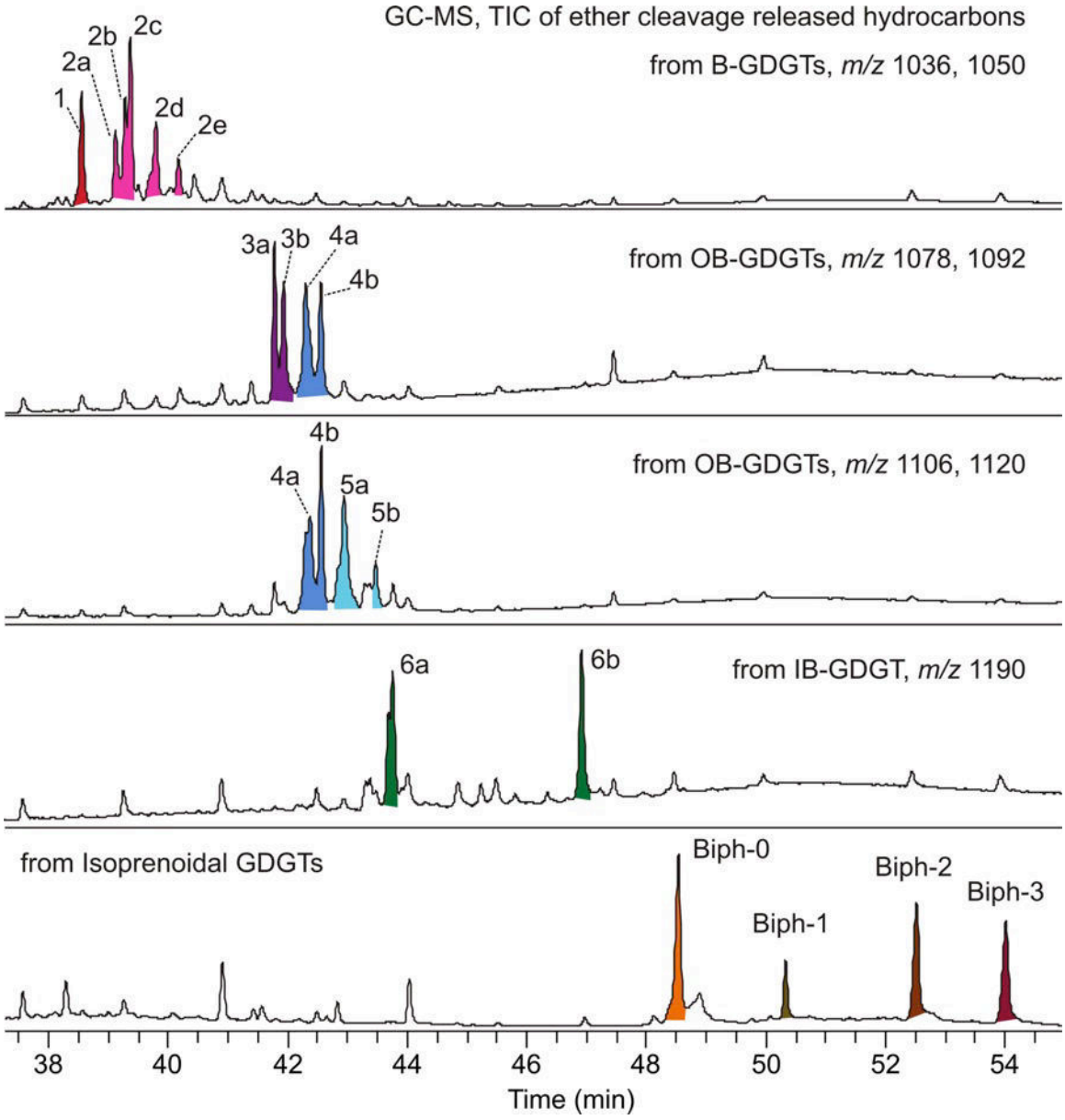

512

513 Fig. 4

514

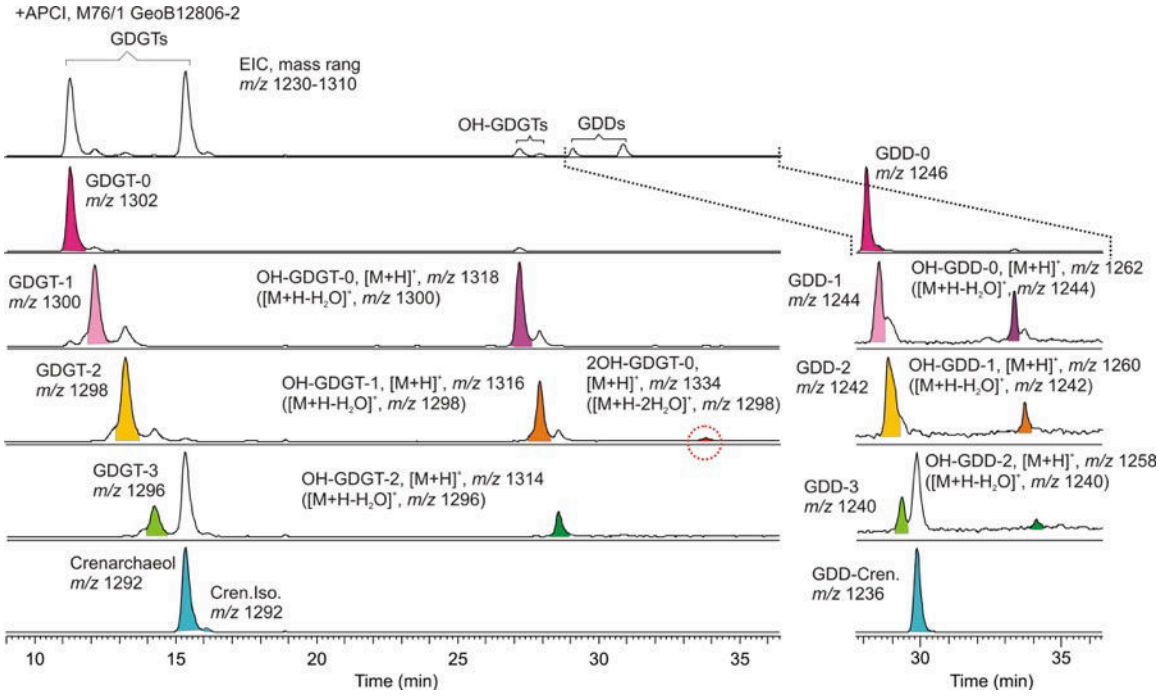

515

516 Fig. 5

517